Research Square

Preprints are preliminary reports that have not undergone peer review.
They should not be considered conclusive, used to inform clinical practice,
or referenced by the media as validated information.

Evaluation of carbon sequestration potential and biogeochemical driving mechanisms in contaminated land under long-term nature-based restoration

I-Chun Chen

cogiitri@gmail.com

Chinese Culture University

Yi-Tang Chang

Soochow University

Research Article

Keywords: Contaminated land, carbon sequestration, nature-based restoration, microbial metabolic, spatial heterogeneity

Posted Date: March 2nd, 2026

DOI: https://doi.org/10.21203/rs.3.rs-8967436/v1

License: This work is licensed under a Creative Commons Attribution 4.0 International License.
Read Full License

Additional Declarations: No competing interests reported.

Abstract

As the global community pursues net-zero emissions by 2050, identifying innovative carbon sinks beyond traditional forest and agricultural sectors has become a strategic imperative. Contaminated land and brownfields represent a significant yet historically overlooked resource for terrestrial carbon sequestration. This study evaluates the capacity of a long-term nature-based restoration project in a cadmium-contaminated agricultural area in Taiwan to function as a verifiable carbon sink. Utilizing high-resolution grid sampling, microbial metabolic profiling with Biolog EcoPlates, and the FAO's EX-Ante Carbon-balance Tool (EX-ACT), the study quantified the cumulative impacts of phytoremediation on soil organic carbon (SOC) and tree biomass carbon stocks. The net carbon balance is governed by a complex interplay among heavy metal toxicity, shifts in microbial functional activity, and rhizosphere priming effects. The results indicate that cadmium stress has been selected for tolerant microbial consortia with high metabolic rates. In addition, rhizosphere priming effects in the subsoil led to trade-offs that enhanced biomass accumulation under specific soil pH, bulk density (BD), electrical conductivity (EC) conditions. This study provides compelling evidence that brownfields possess substantial potential to function as terrestrial carbon sinks through long-term nature-based restoration. Transforming cadmium-contaminated land into a naturalized forest system resulted in a significant net sequestration potential of 4.36 tC/ha/year, driven primarily by vegetation growth. Overall, the regeneration of contaminated land offers a high-performance pathway for carbon sequestration, extending greenhouse gas mitigation benefits beyond those provided by conventional land-use systems.

Introduction

Soil functions as the predominant terrestrial organic carbon repository, sequestering approximately 2,400 gigatons of carbon within the upper two meters of the soil profile, which is nearly three times the amount of carbon stored in the atmosphere (Lal et al., 2021; Lin et al., 2023). Soil organic carbon (SOC) is the foundation of soil health and regulates key chemical and biological processes, serves as a major driver of terrestrial biodiversity, and constitutes the largest terrestrial carbon reservoir. Against the backdrop of the global commitment to achieving net-zero emissions by 2050, the enhancement of SOC has emerged as a central pillar of climate mitigation strategies (Amelung et al., 2020; Crystal-Ornelas et al., 2021; Xu et al., 2020). The significance of this pool is underscored by the "4 per 1000" initiative, which posits that an annual increase of 0.4% in global soil carbon stocks could effectively offset the rise in atmospheric CO_2 (Soussana et al., 2019). This crucial strategic imperative has significantly amplified the urgency and necessity for the exploration and identification of innovative and efficacious carbon sinks that extend beyond the traditional confines of conventional forests and agricultural soils that have historically been relied upon (Yang et al., 2020). However, the inherent challenge associated with the maintenance and enhancement of global SOC stocks is profoundly exacerbated by the pervasive and intensive nature of human activities that systematically undermine the integrity of soil health. (Ngatia et al., 2021) Such anthropogenic pressures systematically contribute to the degradation of soil health, culminating in substantial carbon loss and thereby jeopardizing the essential functions of ecosystems that are vital for environmental sustainability (Morel et al., 2015; Juraev et al., 2024). A comprehensive meta-analysis of

historical trends unequivocally identifies land-use change as a predominant and significant driver of the burgeoning global carbon debt that poses a serious environmental threat. The transformation of natural ecosystems, including but not limited to primary forests and wetlands, into agricultural land has precipitated catastrophic losses of SOC that are alarming in their scope and implications (Sanderman et al., 2017). In tropical regions, for instance, the conversion of pristine primary forests into cropland has resulted in an astonishing loss of SOC stocks ranging from 25% to 30%, a deficit that necessitates a significantly prolonged period for restoration compared to the time required for its initial formation (Beillouin et al., 2023; Xiao et al., 2024). Beyond the detrimental implications of land conversion, the direct pollution of soil presents a multifaceted and enduring threat to the dynamics of soil organic carbon and the overarching health of ecosystems. These contaminant classes rarely exist in isolation; instead, they form a synergistic system of degradation where their co-existence and interaction amplify individual impacts.

Contaminated lands, often referred to as brownfields, represent a vast and frequently overlooked resource in this global effort (Nathanail, 2011; Chen, 2024). These sites, typically idle due to industrial, mining, or waste disposal activities, are often left to undergo natural succession, inadvertently creating conditions conducive to carbon accumulation (Jorat et al., 2020). Understanding and harnessing this potential could offer a dual benefit: remediating environmental hazards while contributing to climate change mitigation (Ancona et al., 2022). It is estimated that 14% to 17% of the world’s croplands are currently affected by heavy metal pollution, while thousands of industrial sites remain idle due to the high costs of conventional remediation (Hou et al., 2025). Historically, these sites have been excluded from carbon sink assessments due to high data uncertainty, complex pollutant-carbon interactions, and the lack of standardized monitoring protocols. Contaminated land has frequently been perceived solely as an environmental liability, representing a significant source of risk that necessitates extensive and costly remediation efforts to restore the land to a usable state (Huang, 2023). However, a paradigm shift is emerging that reframes these sites as potential assets in the fight against climate change. Integrating contaminated sites into carbon management strategies could enhance our understanding of SOC dynamics and promote sustainable land-use practices that benefit both the environment and climate resilience (DiRocco et al., 2014). By transforming contaminated sites into regenerative land, we can align environmental restoration with climate mitigation efforts, ultimately fostering sustainable urban development (Chowdhury et al., 2024; Wan et al., 2024). In the context of national climate goals, such as Taiwan's "Climate Change Response Act," exploring carbon sequestration opportunities on these often-idle lands is a strategic imperative (Chu & Liu, 2021). While international benchmarks provide estimates for carbon sequestration, the transition of contaminated land into a verifiable carbon sink requires a rigorous understanding of the technical methodologies established to meet the guidance from international bodies such as the Intergovernmental Panel on Climate Change (IPCC), the Food and Agriculture Organization (FAO), and voluntary market registries like Verra. These frameworks provide tiered assessment protocols (Tier 1–3) and Monitoring, Reporting, and Verification (MRV) guidelines that ensure the "permanence" and "additionality" of sequestered carbon (Batjes et al., 2024; IPCC, 2019; VCS, 2023; FAO, 2020).

The carbon sink potential of contaminated sites is substantial yet complex (Preston et al., 2020). Emerging research indicates that contaminated sites possess significant, albeit highly variable, carbon sequestration potential (Rumney et al., 2021; Song et al., 2019). This variability is influenced by factors such as soil composition, type of contaminants, and restoration practices employed. Understanding these dynamics is essential for optimizing carbon sequestration in these unique environments (Yuan et al., 2023; Misebo, 2022). While pollution degrades soil health, these often-idle lands also present an opportunity for carbon sequestration if managed correctly. Unmanaged sites undergoing natural succession can passively accumulate significant carbon stocks, with literature values reported at approximately 25 ± 12.8 tC/ha/y (Akala & Lal, 2000; Jorat et al., 2020; Rees et al., 2019). Beyond the assessment of carbon sink on contaminated sites, comparing a complex mixture of plant, animal, and microbial residues at various stages of decomposition is crucial (Kowalska et al., 2020). The presence of pollutants fundamentally alters the intricate biogeochemical processes that govern soil health and carbon storage (Moreno et al., 2009; Mühlbachová et al., 2015). Contaminants do not merely sit inertly in the soil matrix; they actively interact with organic matter, microbial communities, and plant life (Masciandaro et al., 2013; Semple et al., 2007). These interactions disrupt the delicate balance of the soil ecosystem; for example, the microbial degradation of organic pollutants can release carbon, while the toxicity of heavy metals may suppress overall microbial respiration, slowing carbon loss (Chen et al., 2015; Zeng et al., 2024). Consequently, understanding these interactions is vital for developing effective remediation strategies that enhance carbon sequestration while restoring soil health in contaminated environments.

Soil microorganisms are the primary drivers of carbon cycling, and their communities are highly sensitive to pollution (Naylor et al., 2020; Liu et al., 2018; Liu et al., 2023). Contaminant stress can induce significant shifts in microbial community structure and function. For instance, the dominance of K-strategists (e.g., *Actinobacteria*) may be found in long-term pollution, which is adapted to slower growth and the decomposition of more recalcitrant organic matter in soil. The dominance of r-strategists (e.g., *Proteobacteria*) is preferred to thrive on easily decomposable substrates. This shift can alter the rate and pathway of SOC decomposition (Peng et al., 2022; Liu et al., 2018). Contaminants such as cadmium (Cd) and lead (Pb) act as stressors that can inhibit microbial enzyme activity, trigger "priming effects" that accelerate carbon mineralization (Xiao et al., 2024). This heightened activity can accelerate the mineralization of native, stable SOC, leading to a net loss of soil carbon and increased emissions of CO_2 and CH_4. Besides, pollutants disrupt the natural cycle of carbon by altering the balance between carbon inputs from plant matter and carbon outputs via microbial respiration. Heavy metal pollution, for instance, has been shown to reduce overall biodiversity, causing a shift toward communities dominated by a few tolerant species (Qi et al., 2022). This principle of pollution-driven ecological simplification is validated by site-specific empirical evidence (Miao et al., 2025). For instance, in soils contaminated with cadmium, microbial communities have been observed to shift their carbon source utilization primarily toward carbohydrates (Ma et al., 2023; Yan et a., 2024). Furthermore, microbial metabolic activity (measured as Average Well Color Development, AWCD) has shown a positive correlation with soil pH but a negative correlation with organic carbon content, suggesting that under certain contamination pressures, microbial activity may accelerate the mineralization and loss of SOC (Bai et al., 2021; Naz et al., 2022; Zeng et al.,

2024; Xiao et al., 2023). Therefore, each site requires a tailored assessment to determine the relationships between its net potential as a carbon sink and pollutant.

The overarching objective of this study is to systematically evaluate the capacity of long-term contaminated land to function as a significant terrestrial carbon sink. As a result, the study quantifies and establishes a comprehensive, site-specific database of key parameters for analysing the accumulation of SOC and tree biomass carbon in contaminated land in Taiwan. To understand the influence of carbon sequestration in contaminated land under the complex relationships between cadmium (Cd) concentrations, soil physicochemical properties (pH, bulk density, electrical conductivity), and carbon dynamics, this study evaluates the correlations about these parameters to determine how persistent heavy metal stress influences microbial community metabolic profiles and its subsequent impact on SOC mineralization. Finally, this study utilizes the FAO's EX-Ante Carbon-balance Tool (EX-ACT) to simulate the net carbon flux to confirm the potentiality of carbon sequestrations under long-term nature-based restoration conditions.

Materials and methods

Site Description

The investigation was performed at a representative site for soil pollution remediation located in the Delin Section of the Luzhu District in Taoyuan City, Taiwan. The area encompasses approximately 4 hectares and was classified as a general agricultural zone in accordance with Taiwan's National Land Planning Act. In 2004, the Taiwanese government designated two land parcels, numbered 744 and 759, as controlled sites for soil contaminated with cadmium. Then, phytoremediation initiatives were instituted. Figure 1 illustrates aerial imagery depicting the alterations in landscape prior to and following the pollution declaration. In 1995, the region comprised agricultural fields, grasslands, and a single structure. After the pollution declaration in 2005, phytoremediation activities were initiated, accompanied by the construction of three additional buildings. Over time, the afforested areas have developed substantial vegetation density through natural succession. Based on vegetation structure and historical land-use activities, the site was further delineated into five distinct zones, as illustrated in Fig. 2. The green zone signified areas of dense forestation, characterized by low levels of contamination and minimal human intervention. The blue zone denoted areas of significant human activity with irregular forest density. The yellow zone reflected uniform afforestation, elevated contamination, and prior phytoremediation efforts. The brown zone indicated moderate human activity, low forest density, and high levels of contamination. The purple zone represented a diverse species composition, high contamination levels, and natural succession processes. In terms of soil contamination, cadmium concentrations in the topsoil layer (0–15 cm) of the brown and purple zones exceeded Taiwan's regulatory threshold for cadmium in soils used for edible crop production (5 mg/kg). In the yellow zone, cadmium concentrations in both the topsoil (0–15 cm) and subsoil (15–30 cm) exceeded Taiwan's soil cadmium monitoring standard (10 mg/kg), and detectable cadmium contamination persisted at depths of up to 45 cm.

Soil Organic Carbon, Microbial Activity, and Vegetation Investigation

To effectively address the considerable degree of spatial heterogeneity present within the contaminated site, this study employed methodologies encompassing soil organic carbon assessment, evaluation of microbial carbon source metabolic activities, and investigations into vegetation carbon sequestration (FAO, 2020; Rumney et al., 2021; Huang et al., 2024). The 4-hectare experimental area was systematically divided into a grid comprising units of 30 m × 30 m (Fig. 3). A comprehensive total of 30 primary sampling points were established throughout the site in 2025. Soil profiles were evaluated employing a stratified methodology to accurately delineate the distribution of organic carbon at varying depths. Samples were procured from three discrete intervals: 0–15 cm (topsoil), 15–30 cm (subsoil), and from 30 cm to the verified limit of the contamination layer (approximately 45 cm). For the purpose of specific assessments pertaining to carbon stocks, the 15–30 cm and 30–45 cm layers were subsequently amalgamated into a composite subsoil sample, culminating in a total of 60 processed soil samples (30 from topsoil and 30 from subsoil). Reference soil sampling locations were established based on area and the distribution of soil contamination characteristics, resulting in the collection of 32 microbial samples employing the Average Well Color Development (AWCD) method. Vegetation surveys adhered to the principles of plot-based investigation, resulting in the examination of a total of 104 species sampling points. The quantity of investigations conducted in each region is shown in Table 1.

Table 1
Sampling numbers of soil organic carbon, microbial activity, and vegetation growth across investigated zones

Zone	Numbers of Soil sample	Numbers of AWCD	Numbers of Vegetation
Green	12	6	24
Blue	18	10	29
Brown	6	6	15
Purple	6	2	6
Yellow	18	8	30
Total	60	32	104

Laboratory Analysis of Soil Samples

Sampling was conducted at the geometric centroid of each designated grid. In order to ensure horizontal representativeness and to accommodate micro-scale variability, composite samples were created by amalgamating soil retrieved from the primary sampling point and additional locations within a 2-meter radius. The soil bulk density (BD, g/cm^3) was assessed utilizing the non-destructive core method in accordance with NIEA S102.64B, and the samples were weighed in their freshly collected state before

being oven-dried at 105℃ until a stable weight was attained. The gravel content (coarse fragments exceeding 2 mm) was measured by sieving the dried cores through a 10-mesh screen and calculating the mass percentage thereof. The analysis of Total Organic Carbon (TOC) adhered to the combustion/infrared detection methodology (TARI S201.1B), wherein soil samples (0.05–0.1 g) underwent acidification with 1 N HCl using an OI Analytical Aurora 1030s TOC analyzer at a temperature of 900℃. The pH was measured utilizing the compound electrode method (s:w = 1:1) in accordance with NIEA S410.62C. The preparation of saturated soil paste involved the extraction and assessment of soil conductivity using a vacuum pump and a Büchner funnel, referencing the Agricultural Research Institute's "Soil Electrical Conductivity Measurement Method" (TARI S101.1B).

Biolog EcoPlate of Microbial Activity

To investigate the impact of Cd contamination on microbial-mediated carbon cycling, the metabolic potential of the soil microbiome was assessed using Biolog EcoPlates™. AWCD was used as a proxy for the overall metabolic activity and carbon source utilization capacity of the soil microbial communities. 32 samples (representing 16 points at 2 depths) were analyzed for their ability to utilize 31 distinct carbon sources (such as carbohydrates, amino acids, carboxylic acids and polymers). The absorbance was measured at OD_{595} following the redox reaction of tetrazolium violet. The AWCD was calculated using the formula: $AWCD=\sum(Ci - R)/31$, where *Ci* is the absorbance of each well and *R* is the control well absorbance. Higher AWCD values indicate stronger community metabolic activity and greater carbon source utilization potential.

Plot Survey of Tree Carbon Sink

Based on Fig. 3, ascertain the quantity of tree species surveys that were collected for each sample, classified by the various zones, areas exhibiting contamination characteristics, and according to the distinct tree species and sizes that were cultivated; sample surveys were conducted utilizing systematic sampling methodologies for the diverse tree species present in each sample. Approximately 41 distinct tree species were cultivated at this location. The identification of each sample tree species was meticulously documented, including a name tag affixed to the trunk displaying the tree's nomenclature, alongside the diameter at breast height (DBH) of investigated tree using a diameter tape, in addition to the assessment of tree height (H) employing a laser distance measuring device and hypsometer. This study aimed to examine biomass, wood density, carbon content (CF), root-shoot ratio (R) and biomass expansion factor (BEF) for reference purposes in Taiwan, with the objective of constructing a comprehensive database of parameters for estimating the carbon stock of soil conservation tree species. Approximately 4000 trees were cultivated across 30 samples, resulting in the establishment of a database encompassing 104 trees with various parameters.

Soil Organic Carbon Stock Calculation

The soil organic carbon density (SOCD) quantified in kilograms of carbon per square meter (kg C/m²) was determined for a singular soil depth layer. The SOCDi was computed utilizing the formula.

$SOCD_i = SOC_i \times \rho_i \times d_i \times (1 - CF_i\ \%)/\ 100$ (1)

where $SOCD_i$ and SOC_i represent the SOC density (kg/cm²) and concentration (g/kg) of the ith layer, respectively; ρ_i denotes the soil bulk density of the ith layer (g/cm³); d_i indicates the depth of the ith layer (cm); and CF_i is the percentage (%) of coarse fragments exceeding 2 mm in the ith layer; the constant 100 serves as a conversion factor.

For the distinct profiles with a specified depth (D), SOC densities were derived by aggregating the SOC density across each soil layer corresponding to various zones. Ultimately, the SOC stock within each soil depth layer of the examined grid was estimated by multiplying the SOC density within each unit area (kg C/m²) by the total area (S_j) encompassed by each grid. The cumulative SOC stocks across each depth layer yield the comprehensive SOC stock within each investigated grid. Consequently, the overall SOC storage is computed through the summation of $SOCD_i$ (the mean SOC density of the jth investigated grid) and S_j, which refers to the total area (m²) of a specific investigated grid j within the studied region.

Tree Carbon Stock Calculation

The current investigation employed the biomass assessment formula for topsoil developed by Chave in 2014, which was deemed appropriate for the evaluation of tropical tree species prevalent in common wetland conservation areas within Taiwan, and was likewise examined at the designated study site. In accordance with the assessment principle established by the IPCC, the vegetation carbon content associated with tree species must encompass both aboveground and subsoil biomass, in addition to the BEF. This research formulated the estimation for tree species in year t stratification j utilizing the formula.

$GW_{i,j,t}=0.0673\times(p\times DBH^2\times H)^{0.976}\times BEF\times(1 + R)\times CF$ (2)

where ρ denotes the wood density (g/cm^3), BEF represents the biomass expansion factor, R signifies the rhizome ratio, and CF indicates the carbon content (%). The cumulative tree carbon stock within the research area was quantified as the aggregate of $GW_{i,j,t}$ multiplied by $N_{i,j,t}$, wherein $N_{i,j,t}$ reflects the count of tree species within tier i during year t.

Data Statistics

To verify the precision of the carbon baseline for potential entry into international carbon markets (e.g., Verra), the Minimum Detectable Difference (MDD) was calculated at a 95% confidence level (t = 2.045). The MDD provided a statistical threshold for detecting significant changes in carbon sequestration over future verification cycles, typically requiring values between 0.05% and 0.2% for high-quality carbon credits. The MDD served to validate the appropriateness of the sampling density employed in this study.

$$MDD \geq \frac{S}{\sqrt{n}} \times (t_{a,v} + t_{\beta,v}) \quad (3)$$

Comprehensive statistical methodology and visualization outcomes were utilized to integrate interrelations among pollutants, carbon reserves, and microbial activity. The Pearson and Spearman correlation coefficients were computed to ascertain the intensity of correlations among soil pH, bulk density (BD), electrical conductivity (EC), organic carbon percentage (OC%), total inorganic carbon percentage (TIC%), arboreal carbon stock, and average well color development (AWCD) values. Furthermore, Principal Component Analysis (PCA) was particularly employed to assess the functional metabolic diversity of microorganisms and to distinguish the metabolic profiles of soil microbial communities within the context of this investigation. Ascertain the loading scores corresponding to each of the 31 carbon substrates. This analysis facilitates the identification of which particular nutrients (such as amino acids, carboxylic acids, or carbohydrates) are paramount for differentiating the communities. Ultimately, the results represent the samples within a two-dimensional coordinate framework (PC1 versus PC2). Examine how various provenances (for instance, high versus low carbon sequestration) cluster or disperse to elucidate the principal factors affecting their functional diversity.

Integrated Carbon Balance Scenarios

This study employed the Food and Agriculture Organization's EX-ante Carbon-Balance Tool (EX-ACT) as its principal analytical instrument. The methodology for calculations adhered to the guidelines established by the IPCC for assessing the carbon balance associated with afforestation and reforestation activities. By employing aerial imagery, the study elucidated the consequences of land use alterations across distinct temporal markers, specifically before and after the initiation of the phytoremediation program, following site contamination as reported by governmental declarations. Furthermore, it evaluated the implications for carbon balance resulting from modifications in the land management strategy initiated in 1995, the initiation of capitalization in 2005, and the land survey conducted in 2025. In addition to integrating data pertaining to soil organic carbon stock and the carbon reserves associated with the planting of phytoremediation trees, this study also acquired information on activities contributing to greenhouse gas emissions from land management practices via interviews with landowners. These practices encompassed agricultural cultivation and tillage methods, the frequency of agricultural waste incineration, annual fertilization methodologies and their respective occurrences, as well as rates of tree damage and degradation, among other factors. Ultimately, the research assessed the aggregate carbon emissions that result from the implementation of the restoration plan following the pollution announcement at the specified site.

Carbon dynamics were simulated based on three temporal scenarios derived from site history and landowner interviews:

- **Scenario X0**: Initial condition (prior to 1995) representing conventional rice paddy management.
- **Scenario X1**: Transitional period (post-2005) where the site underwent phytoremediation following the discovery of contamination.
- **Scenario X2**: Current intervention state characterized by natural forest succession and low-intensity management.

Results and Discussion

Responses of Microbial Functional Activity and Carbon Stocks Coupling to Pollution Intensity

The site undergoing phytoremediation presents complex interactions between soil structure, organic matter, and contamination levels in this study. Figure 4 presents that Cd concentration in topsoil is positively correlated with BD, potentially reflecting the accumulation of contaminants more compacted in the topsoil (0–15 cm). The phenomenon also verified the positive correlations (r = 0.65) between soil pH and electrical conductivity (EC) in topsoil to improve the condition, that microbial metabolic activity often shows a positive correlation with soil pH, which is supported by the observed topsoil correlation between pH and AWCD (r = 0.22). The impact of cadmium on microbial functional diversity is multifaceted. While heavy metals are generally toxic, long-term exposure can lead to the selection of tolerant species. Soil pH plays a critical role in regulating the bioavailability of heavy metals. In this study, the condition of soil pH in topsoil limited the contamination transportation that the microbial communities dominated then accelerated the mineralization of SOC. As a result, the findings show that the correlation between Cd concentration and AWCD is weakly positive (r = 0.16) in the topsoil. This may reflect a "priming effect" where cadmium-induced stress triggers a shift in microbial community structure toward tolerant populations that maintain high metabolic rates despite the presence of contaminants. Furthermore, the potentially localized SOC mineralization of native SOC in topsoil resulting from microbial activity causes the negative correlation between Cd concentration and OC (r = -0.21) and the toxicity of cadmium remains a significant inhibitory factor for vegetation growth, which in turn limits the input of fresh organic matter into the soil system.

However, Fig. 5 presents that the relationship between Cd and AWCD becomes slightly negative (r = -0.08) in the subsoil (15–45 cm). This suggests that the adapted tolerance microbial communities observed in the topsoil may not be as prevalent in deeper layers, where lower oxygen levels and different nutrient availability might exacerbate the toxic effects of cadmium on microbial respiration. Moreover, the finding indicates that AWCD shows a negative correlation with BD (r = -0.50) and the soil compaction acts as a physical barrier that restricts microbial access to oxygen and nutrients, thereby suppressing overall metabolic potential. The phenomenon is verified as the negative correlation (r = -0.50) between AWCD and BD. Furthermore, the correlation weakens considerably (r = 0.10) indicates that deeper soil layers are influenced by different physical and biological drivers because of the positive correlation between OC and

BD in general. In addition, tree carbon stock has a negative correlation with OC percentage (r = -0.61) and this trend is even more pronounced in the subsoil. This strong negative correlation between arboreal biomass and soil organic carbon in deeper layers suggests a significant "rhizosphere priming effect". Higher vegetation density generally increases microbial biomass, diversity, carbon-cycling enzymes, and mineralization of SOC, partly through increased plant carbon and nutrient inputs. More roots particularly improve the decomposition of more complex substrates (such as leaf litter and lignin-rich material) while having little effect on simple substrates, consistent with microbes using root carbon to present the decomposition of SOM. This mechanism highlights a critical trade-off at the Luzhu site. Consequently, the phytoremediation effort has enhanced not only the carbon reserves within aboveground biomass but also the microbial biomass in the soil stemming from cadmium-tolerant microbial consortia, particularly in reducing the mineralization of soil organic carbon in the subsoil.

To comprehend the reciprocal impact of varied regional pollution attributes on vegetation growth, soil organic carbon, and soil microbiota in the rhizosphere, the current investigation assessed the AWCD, as shown in Table 2, indicating that pollution characteristics are responsible for the promotion of cadmium-resistant microbial proliferation at a cadmium concentration of 6.16 mg/kg alongside a comparatively elevated AWCD value of 0.61. Soil microorganisms endemic to the study locale have not been suppressed by prolonged cadmium exposure. Conversely, Table 2 elucidates that samples area 2 and area 3 exhibit diminished cadmium concentration in sample 2 (cadmium concentration: 1.57 mg/kg), yet manifest substantial Tree carbon stock values (5.83 tons), which are inferior to the Tree carbon stocks observed in sample zone 3 (1.92 tons). Furthermore, AWCD values in sample area 2 are markedly higher than those in sample 3, signifying that soil microbiota's carbon utilization is predominantly influenced by terrestrial biocarbon solid carbon capacity, thereby enhancing microbial activity within the rhizosphere. Figure 6 shows the PCA profile of each area sample in Table 2. Interestingly, most samples (A3/B3, A9/B9, and A16/B16) in area 1 present similar utilization on the PCA profile between topsoil and subsoil samples in the lowest soil carbon stock (32.72 tC/ha) and the highest tree carbon stocks (10.17 tC). Previous studies present that high diversity of trees can increase microbial growth (biomass), enzyme activity, and microbial carbon use efficiency (CUE), especially in carbon-rich topsoil (Duan et al., 2023). Specific tree species with high-quality litter (such as arbuscular mycorrhizal-associated trees) had higher microbial biomass and less nutrient limitation that were conducive to higher decomposition rates and lower carbon stocks in the forest floor. Such tree species could lead to both greater stabilization of mineral soil C by mineral-associated OM formation and greater microbial mineralization of SOM with higher microbial resource demand (Salome et al., 2010). However, most samples (A18, A29, and A23) on the PCA profile belong to the topsoil in area 4, with the highest soil carbon stock (69.72 tC/ha) and the lowest tree carbon stocks (0.61 tC). Area 4 presents a high concentration of SOC, microorganisms, and biological activity in the topsoil, leading to the highest AWCD value (0.61) in the profile. Table 3 reveals that soil microorganisms in area 2, with the lowest cadmium contamination (1.57 mg/kg), serve as the primary carbon sources for carbohydrates, including D-cellobiose, D-Galacturonic acid lactone, and Methy-1-D-glucoside. Soil microorganisms in area 1, with the medium cadmium contamination (3.19 mg/kg), predominantly utilize carbon resources on Biolog Ecoplates, including N-acetyl-D-glucosamine in carboxylic acids, γ-Hydroxy butyric acid in carboxylic acids, L-phenylalanine in amino acids, and Tween 40 in polymers. Besides, soil microorganisms in area 4, with

the highest cadmium contamination (6.16 mg/kg), utilize specific amino acids: L-Asparagine and Glycyl-L-glutamic acid. Metagenomic and predictive functional profiling in heavy metal-contaminated agricultural soils can enhance their potential ecological functions under stress. For example, an enrichment of carbohydrate metabolism pathways alongside membrane transport and energy metabolism is detected as being consistent with adjusting their composition (Liu et al., 2024). Soil microbial communities are selectively taking up different substrates, influenced by the physicochemical characteristics of heavy metals. AWCD showed a consistent trend in mining-contaminated arid soils, contaminated by As and heavy metals: carbohydrates > polymers > carboxylic acids > amino acids > amines/amides as carbon sources (Martínez-Toledo et al., 2021). The existing literature indicates that cadmium-tolerant soil microorganisms primarily consist of *Nitrospirae*, *Firmicutes*, and *Verrucomicrobia*, with *Bacillus spp. 6–6* being well-suited for carbohydrate degradation derived from plant residues and rootstocks, such as *Bacillus sp. 6–6* (Ma et al., 2023; Yan et al., 2024). Although microbiome sequencing was not conducted in this investigation, the correlational analysis concerning the relationship with AWCD values from diverse soil baseline data implies the presence of cadmium-tolerant soil microorganisms at the site, and demonstrates that an increase in Tree carbon stocks correlates with elevated AWCD values, which may also contribute to an enhancement in the rates of soil organic mineralization, hence AWCD values exhibit a negative correlation with organic carbon (OC) values.

Table 2
The comparative data of the carbon stocks (soil and tree) and AWCD under the different concentration

Area	Sampling Number	Cd Concentration (mg/kg)	Soil Carbon Stocks (tC/ha)	Tree Carbon Stocks (tC)	AWCD
1	3, 9, 14, 16, 17	3.19	37.72	10.17	0.40
2	2, 7, 8	1.57	62.17	5.83	0.47
3	6, 12	2.80	63.05	1.92	0.17
4	18, 21, 23, 29	6.16	69.72	3.22	0.61

Table 3
PCA loading scores for the 31 Biolog carbon substrates across the investegated area

Carbon Type	Feature	Area 1		Area 2		Area 3		Area 4	
		PC1	PC2	PC1	PC2	PC1	PC2	PC1	PC2
Carbohydrates	Methyl-D-glucoside	-0.11	-0.05	0.29	0.12	0.01	0.03	-0.06	-0.26
Carbohydrates	D-Galactonic acid lactone	-0.17	0.33	0.35	0.05	-0.01	0.00	-0.15	-0.37
Amino acids	L-Arginine	0.00	-0.25	-0.08	0.07	-0.27	-0.50	-0.10	0.39
Carboxylic acids	Pyruvic acid methyl ester	-0.15	-0.10	-0.17	0.21	-0.85	0.36	0.42	0.07
Carbohydrates	D-Xylose	-0.03	0.03	0.00	0.01	0.02	0.04	-0.02	-0.03
Carbohydrates	D-Galacturonic acid	-0.06	-0.18	0.19	-0.48	0.23	0.09	0.68	-0.26
Amino acids	L-Asparagine	0.04	-0.47	-0.22	0.14	-0.18	-0.38	0.44	0.36
Polymers	Tween 40	0.13	-0.13	-0.43	0.04	0.11	0.07	-0.17	0.18
Carbohydrates	i-Erythritol	0.00	0.06	-0.01	0.02	-0.03	0.01	0.00	0.00
Phenolic acid	2-Hydroxy benzoic acid	-0.05	0.00	0.00	-0.03	-0.01	-0.01	-0.02	-0.01
Amino acids	L-Phenylalanine	0.16	-0.20	-0.19	-0.33	0.01	0.10	-0.06	0.34
Polymers	Tween 80	-0.04	0.08	-0.13	0.12	0.08	-0.13	-0.04	-0.09
Carbohydrates	D-Mannitol	-0.08	-0.11	-0.36	-0.07	0.21	-0.09	-0.17	0.14
Phenolic acid	4-Hydroxy benzoic acid	-0.09	-0.22	0.08	0.27	0.01	0.00	-0.10	0.04
Amino acids	L-Serine	-0.12	0.21	0.12	0.05	0.00	0.00	-0.10	-0.25
Polymers	α-Cyclodextrin	0.00	0.02	0.00	0.03	-0.02	0.03	0.00	0.00
Carbohydrates	N-Acetyl-D-glucosamine	0.79	0.32	0.02	-0.38	0.11	0.02	-0.12	-0.01
Carboxylic acids	γ-Hydroxy butyric acid	0.31	0.04	-0.17	0.05	0.15	0.63	-0.08	0.32
Amino acids	L-Threonine	-0.04	-0.03	0.00	-0.02	0.01	-0.03	0.00	-0.04
Polymers	Glycogen	0.02	0.00	0.17	0.11	0.05	0.10	0.03	0.06
Carbohydrates	D-Glucosaminic acid	-0.03	0.03	0.09	-0.14	-0.05	0.06	-0.06	0.00

Carbon Type	Feature	Area 1		Area 2		Area 3		Area 4	
		PC1	PC2	PC1	PC2	PC1	PC2	PC1	PC2
Carboxylic acids	Itaconic acid	0.03	0.07	-0.06	-0.36	0.05	0.03	-0.06	-0.16
Amino acids	Glycyl-L-glutamic acid	-0.01	0.04	-0.01	0.06	-0.02	0.05	0.05	-0.05
Carbohydrates	D-Cellobiose	-0.02	0.02	0.36	0.13	0.03	0.08	-0.04	-0.07
Carbohydrates	Glucose-1-phosphate	-0.04	0.03	0.12	0.07	-0.08	0.06	-0.02	-0.01
Carboxylic acids	α-Keto butyric acid	0.03	0.04	-0.01	-0.02	-0.01	0.00	-0.02	0.01
Amines	Phenylethylamine	-0.06	-0.07	0.12	-0.09	0.04	-0.01	-0.03	0.04
Carbohydrates	α-D-Lactose	-0.01	0.02	0.00	0.01	-0.01	0.01	-0.01	0.01
Carbohydrates	D,L-α-Glycerol phosphate	-0.03	-0.04	-0.18	0.31	0.02	0.05	-0.06	-0.07
Carboxylic acids	D-Malic acid	-0.06	-0.02	-0.03	-0.11	0.05	0.04	-0.04	-0.10
Amines	Putrescine	-0.34	0.52	0.13	0.19	0.01	0.00	-0.08	-0.20

Spatial Heterogeneity of Carbon Stocks

To evaluate the existence of spatial heterogeneity in soil organic carbon in this study, MDD analysis was conducted using 16 samples collected within the same geographical area, with sampling intervals exceeding two months. The outcomes of the analysis indicate that the MDD values recorded are 0.96% and 0.83% in the green and purple zones, respectively, reflecting the influences of low and high pollution levels on the spatial variability of soil carbon stocks. Under measurement, reporting, and verification (MRV) guidelines for soil carbon credit assessment, acceptable thresholds typically range from 0.3% to 0.5%. The observed MDD values exceed these thresholds, indicating pronounced spatial heterogeneity in SOC at the study site and underscoring the necessity of high-resolution sampling for reliable SOC assessment.

The findings indicate that soil carbon stocks in regions characterized by elevated pollution levels exceed those in regions with diminished pollution levels. Figure 7 illustrates that carbon stocks within the yellow zone situated to the south of the site may attain levels of 79.97 tC/ha (sampling point 23) and carbon stocks in the purple zone are recorded at 96.16 tC/ha (sample point 21). These deposits of soil organic carbon result from the microbiological suppression under the upper stratum of the soil and the contamination by cadmium originating from the topsoil. Conversely, these two regions exhibit elevated bulk density values of topsoil and subsoil in comparison to other areas, resulting in impediments to the growth of soil microbiota due to the compaction of the soil. This phenomenon has been corroborated by the AWCD values, which indicates a deceleration in the rate of soil mineralization.

In addition, the results also substantiate the influence of soil deposition as evidenced by the bulk density (BD) measurements of both the topsoil and subsoil layers. Figure 7 illustrates that the comparatively lower concentration of soil carbon stocks on the northern area of the site is elevated (72.67 tC/ha), which results in diminished microbial proliferation attributable to the reduced BD value observed in the topsoil of that particular region. The BD value in typical soils may exhibit an increase with increasing soil depth. In instances where the differential is positive, it signifies that the BD values are higher than the topsoil subsequent to the stabilization of soil aggregates over time. Should the discrepancy between the two values exceed 0.6, it indicates that the surface soil is influenced by anthropogenic disturbances (e.g., tillage), whereas in areas characterized by nature-based restoration, the variation falls within the range of 0.2 to 0.4. Figure 8 presents a BD difference ranging from − 0.02 to 0.34, with a mean value approximating 0.2, thereby suggesting that the research site has remained undisturbed by human activities. The difference is represented as a negative value due to an elevated BD value in the topsoil, which may precipitate soil degradation as a consequence of pollution that inhibits microbial proliferation.

Alterations in soil conductivity significantly influence the translocation of heavy metals, concomitantly affecting the microbial activity within the rhizosphere. Consequently, this research uses a comprehensive analysis of soil conductivity across 30 designated sampling points within the study area. Under typical environmental conditions, characterized by specific climatic factors and soil leaching dynamics, conductivity is observed to increase with depth, whereby subsurface conductivity exceeds that of surface soil conductivity, yielding a positive differential. Figure 9 illustrates the in-situ soil conductivity ranging from − 0.18 to 0.24. A predominant observation throughout the site indicates that surface soil conductivity surpasses that of subsurface conductivity, resulting in a negative differential. The findings suggest that the surface soil within the site facilitates the mobilization of pollutants under conditions of elevated conductivity. In contrast, electrical conductivity in the subsoil layer of the southern portion of the site exceeded that of the topsoil. This condition may promote the proliferation of cadmium-resistant microorganisms in the subsoil rhizosphere, thereby potentially enhancing overall microbial resilience and supporting plant growth under contaminated conditions. Figure 10 presents data pertaining to the highest tree carbon stocks in this locality (sampling point 19), with an estimated mass of 199 tonnes of tree carbon stocks.

Site-level Carbon Balance and Sequestration Potential

This study employs aerial imagery and interviews with landowners to ascertain the historical transformations in land use and the corresponding greenhouse gas (GHG) emissions resulting from activities within the site. The FAO-developed EX-Ante Carbon-balance Tool is utilized to evaluate the carbon balance and carbon sequestration potential of the site before and after the implementation of the project in 2004. Prior to the execution of the project, the land use consisted of degraded agriculture land and grassland, with approximately thirty deer being raised within the site. Following the project implementation, artificial afforestation was conducted to facilitate ecological restoration and phytoremediation, utilizing agroforestry and multistrata planting techniques. This study employs the stock change factor for mineral soil organic carbon land-use systems or sub-systems (Flu) as established by the

IPCC, in conjunction with the default values for biomass of aboveground vegetation, and utilizes the SOC values previously surveyed by the Taiwan Agricultural Research Institute (TARI) in the region as a baseline for carbon sequestration and emission conditions associated with the initial land use type. Concurrently, the investigation of the current site conditions included the measurement of soil carbon stocks and tree carbon stocks, which serve as parameters for carbon input in the post-restoration land use type. Moreover, data pertaining to the mean annual temperature (MAT), mean annual precipitation (MAP), and potential evapotranspiration (PET) are collected from the IPCC database to corroborate the climatic conditions of the site. The results indicate that the site achieved a net carbon balance of 1,919 tCO_{2e}, driven by land management, vegetation changes, and the elimination of livestock activities. This corresponds to a negative carbon sequestration potential of approximately 479.7 tCO2e/ha, equivalent to an average annual carbon sink of about 16 tCO_{2e}/ha/year (4.36 tC/ha/year), as shown in Fig. 11. The negative carbon effect stemming from vegetation changes was the most significant, totaling 1,114 tCO_{2e}. The carbon sequestration effect over a 30-year period is approximately 9.6 tCO_{2e} /ha/year attributed to the growth of robust carbon-storing plantings, whereas the sequestration of carbon in soil is quantified at 3 tCO_{2e} /ha/year. The cessation of livestock agriculture yields a reduction in carbon emissions estimated at 3.4 tCO_{2e} /ha/year. As a result, the potential for carbon pooling through long-term plant-based regeneration and natural methodologies aimed at redeveloping contaminated land is indeed substantial.

Conclusions

The study provides compelling evidence that brownfields possess substantial potential to contribute to global net-zero objectives through natural succession and phytoremediation. The investigation at the Luzhu District site demonstrates that transforming a cadmium contaminated land into a naturalized forest system resulted in a net carbon balance of 1,919 tCO_{2e}, representing a significant negative carbon sequestration potential of approximately 4.36 tC/ha/year. Vegetation growth contributed a net negative carbon balance of 1,114 tCO_2e, indicating that robust soil conservation plantings can sequester carbon at an estimated rate of approximately 9.6 tCO_{2e} /ha/year. This highlights the efficacy of using phytoremediation not only for pollutant stabilization but also as a high-performance nature-based solution for carbon capture. Moreover, a weak positive correlation between Cd concentration and AWCD suggests that long-term exposure may have been selected for cadmium-tolerant microbial consortia. These adapted populations may heighten metabolic activity accelerated the mineralization of native SOC in the topsoil layer and PCA reveals a distinct functional shift, that the microbial communities in high-contamination zones prioritized carbohydrate utilization, whereas low-pollution regions relied on carboxylic acids. The findings underscore some critical insights including the most significant contributions of carbon sink by the transition in vegetation from the long-term phytoremediation, the sophisticated interaction between cadmium stress and microbial carbon cycling, the consideration of the high degree of spatial heterogeneity inherent in brownfield, and the soil structure changes under long-term and natural succession.

In summary, this study validates that the long-term nature-based regeneration of contaminated land offers a dual benefit including the remediation of environmental hazards and the creation of substantial carbon

pools. Building on these findings, continuous data collection and long-term monitoring are required at other contaminated sites to improve the accuracy and verification credibility of soil carbon sequestration assessments in Taiwan.

Declarations

Author Contribution

I.-C. Chen Conceptualization, Methodology, Software, Validation, Formal analysis, Resources, Writing - Editing, Visualization, Funding acquisition, Supervision, Project administration. Y.-T. Chang Writing – Review, Data curation, Formal analysis.

Acknowledgements

The authors gratefully acknowledge financial support from the 2024 research grant of the Soil and Groundwater Pollution Remediation Fund, Taiwan.

References

1. Akala, V. A., & Lal, R. (2000). Potential of mine land reclamation for soil organic carbon sequestration in Ohio. Land Degradation & Development, 11(3), 289–297. https://doi.org/10.1002/1099-145X(200005/06)11:3%3C289::AID-LDR385%3E3.0.CO;2-Y
2. Amelung, W., Amelung, W., Bossio, D. A., Vries, W. de, Kögel-Knabner, I., Lehmann, J., Lehmann, J., Amundson, R., Bol, R., Collins, C., & Lal, R. (2020). Towards a global-scale soil climate mitigation strategy. Nature Communications, 11(1), 5427. https://doi.org/10.1038/S41467-020-18887-7
3. Ancona, V., Rascio, I., Aimola, G., Barra Caracciolo, A., Grenni, P., Uricchio, V. F., & Borello, D. (2022). Plant-assisted bioremediation: Soil recovery and energy from biomass. Assisted Phytoremediation, 25–48. https://doi.org/10.1016/B978-0-12-822893-7.00012-4
4. Bai, X.-T., Wang, J., Dong, H., Chen, J.-M., & Ge, Y. (2021). Relative importance of soil properties and heavy metals/metalloids to modulate microbial community and activity at a smelting site. Journal of Soils and Sediments, 21(1), 1–12. https://doi.org/10.1007/S11368-020-02743-8
5. Beillouin, D., Corbeels, M., Demenois, J., Berre, D., Boyer, A., Fallot, A., Feder, F., & Cardinael, R. (2023). A Global Meta-Analysis of Soil Organic Carbon in the Anthropocene. Nature Communications, 14. https://doi.org/10.1038/s41467-023-39338-z
6. Batjes, N. H., Ceschia, É., Heuvelink, G. B. M., Demenois, J., Maire, G. L., Cardinael, R., Arias-Navarro, C., & Egmond, F. van. (2024). Towards a modular, multi-ecosystem monitoring, reporting and verification (MRV) framework for soil organic carbon stock change assessment. Carbon Management, 15(1). https://doi.org/10.1080/17583004.2024.2410812
7. Chave, J., Réjou-Méchain, M., Búrquez, A., Chidumayo, E., Colgan, M. S., Delitti, W. B. C., Duque, A., Eid, T., Fearnside, P. M., Goodman, R. C., Henry, M., Martínez-Yrízar, A., Mu gasha, W. A., Muller-Landau, H.

C., Mencuccini, M., Nelson, B. W., Ngomanda, A., Nogueira, E. M., Ortiz-Malavassi, E., … Vieilledent, G. (2014). Improved allometric models to estimate the aboveground biomass of tropical trees. Global Change Biology, 20, 3177–3190.

8. Chen, Y., Liu, Q., Liu, Y. J., Jia, F. A., & He, X. (2015). Responses of soil microbial activity to cadmium pollution and elevated CO2. Scientific Reports, 4(1), 4287–4287. https://doi.org/10.1038/SREP04287
9. Chen, I.-C. (2024). Predicting regional sustainable development to enhance decision-making in brownfield redevelopment using machine learning algorithms. Ecological Indicators, 112117.
10. Chowdhury, S. N., Volchko, Y., & Norrman, J. (2024). A Framework for Upgrading Contaminated Urban Land and Soil by Nature-Based Solutions: Demonstration with a Swedish Case. Urban Science. https://doi.org/10.3390/urbansci8040198
11. Chu, M.-Y., & Liu, W.-Y. (2021). Assessing the Opportunity Cost of Carbon Stock Caused by Land-Use Changes in Taiwan. Land, 10(11), 1240. https://doi.org/10.3390/LAND10111240
12. Crystal-Ornelas, R., Thapa, R., & Tully, K. L. (2021). Soil organic carbon is affected by organic amendments, conservation tillage, and cover cropping in organic farming systems: A meta-analysis. Agric. Ecosyst. Environ., 312, 107356. https://doi.org/10.1016/j.agee.2021.107356
13. DiRocco, T. L., Ramage, B. S., Evans, S. G., & Potts, M. D. (2014). Accountable Accounting: Carbon-Based Management on Marginal Lands. Forests, 5(4), 847–861. https://doi.org/10.3390/F5040847
14. Duan, P., Fu, R., Nottingham, A. T, Domeignoz-Horta, L. A., Yang, X., Du, H., Wang, K., & Li ,D. (2023). Tree species diversity increases soil microbial carbon use efficiency in a subtropical forest. Glob Chang Biol., 29(24), 7131–7144. https://doi.org/10.1111/gcb.16971
15. Hou, D. (2025). Global soil pollution by toxic metals threatens agriculture and human health. Science, 388, 316–321. https://doi.org/10.1126/science.adr5214
16. FAO. A protocol for measurement, monitoring, reporting and verification of soil organic carbon in agricultural landscapes – GSOC-MRV Protocol (p. 140). (2020). FAO, ITPS, GSP.
17. Huang, Z. (2023). Analysis of Carbon Sequestration Capacity in Land Remediation Projects. Frontiers in Sustainable Development, 3(9), 1–5. https://doi.org/https://doi.org/10.54691/fsd.v3i9.5594
18. Huang, Z., Qin, Y., He, X., Zhang, M., Ren, X., Yu, W., & Ji, K. (2024). Analysis on metabolic functions of rhizosphere microbial communities of Pinus massoniana provenances with different carbon storage by Biolog Eco microplates. Front. Microbiol., 15, 1365111. https://doi.org/10.3389/fmicb.2024.1365111
19. Intergovernmental Panel on Climate Change. (2019). Chapter 2: Generic Methodologies Applicable to Multiple Land-Use Categories. In 2019 Refinement to the 2006 IPCC Guidelines for National Greenhouse Gas Inventories: Volume 4 – Agriculture, Forestry and Other Land Use (Vol. 4). IPCC.
20. Jorat, M. E., Jorat, M. E., Goddard, M. A., Goddard, M. A., Manning, P., Lau, H. K., Ngeow, S., Sohi, S., & Manning, D. A. C. (2020). Passive CO2 removal in urban soils: Evidence from brownfield sites. Science of The Total Environment, 703, 135573. https://doi.org/10.1016/J.SCITOTENV.2019.135573
21. Juraev, Z., Ahn, Y.-J., & Koriyev, M. (2024). Urban Soil Dynamics: The Relationship Between Soil Health and Urbanization. Deleted Journal, 3(2), 62–69. https://doi.org/10.36777/jag2024.3.2.6

22. Kowalska, A., Pawlewicz, A., Dusza, M., Jaskulak, M., & Grobelak, A. (2020). Plant–soil interactions in soil organic carbon sequestration as a restoration tool. 663–688. https://doi.org/10.1016/B978-0-12-818032-7.00023-0
23. Lal, R., Monger, C., Nave, L., Nave, L., & Smith, P. (2021). The role of soil in regulation of climate. Philosophical Transactions of the Royal Society B, 376(1834), 20210084. https://doi.org/10.1098/RSTB.2021.0084
24. Lin, Z.-Y., Dai, Y., Mishra, U., Wang, G., Shangguan, W., Zhang, W., & Qin, Z. (2023). Global and Regional Soil Organic Carbon Estimates: Magnitude and Uncertainties. Pedosphere. https://doi.org/10.1016/j.pedsph.2023.06.005
25. Liu, J., Pei, S., Zheng, Q., Li, J., Liu, X., Ruan, Y., Luo, B., Ma, L., Chen, R., Hu, W., Niu, J., & Tian, T. (2024). Heavy metal contamination impacts the structure and co-occurrence patterns of bacterial communities in agricultural soils. J Basic Microbiol., 64(3), e2300435. https://doi.org/10.1002/jobm.202300435
26. Liu, X., Xu, X., & Ma, T. (2023). Linking microbial carbon pump capacity and efficacy to soil organic carbon storage and stability under heavy metal pollution. Soil Ecol. Lett., 5, 220140. https://doi.org/10.1007/s42832-022-0140-8
27. Liu, Y.-R., Delgado-Baquerizo, M., Delgado-Baquerizo, M., Wang, J.-T., Hu, H.-W., Yang, Z., He, J.-Z., & He, J.-Z. (2018). New insights into the role of microbial community composition in driving soil respiration rates. Soil Biology & Biochemistry, 118, 35–41. https://doi.org/10.1016/J.SOILBIO.2017.12.003
28. Ma, B., Song, W., Zhang, X., Chen, M., Li, J., Yang, X., & Zhang, L. (2023). Potential application of novel cadmium-tolerant bacteria in bioremediation of Cd-contaminated soil. Ecotoxicology and Environmental Safety, 255, 114766. https://doi.org/10.1016/j.ecoenv.2023.114766
29. Martínez-Toledo, Á., González-Mille, D. J., García-Arreola, M. E., Cruz-Santiago, O., Trejo-Acevedo, A., & Ilizaliturri-Hernández, C. A. (2021). Patterns in utilization of carbon sources in soil microbial communities contaminated with mine solid wastes from San Luis Potosi, Mexico. Ecotoxicology and Environmental Safety, 208, 111493. https://doi.org/10.1016/j.ecoenv.2020.111493
30. Masciandaro, G., Macci, C., Peruzzi, E., Ceccanti, B., & Doni, S. (2013). Organic matter–microorganism–plant in soil bioremediation: a synergic approach. Reviews in Environmental Science and Bio/Technology, 12(4), 399–419. https://doi.org/10.1007/S11157-013-9313-3
31. Miao, Y., Zhou, D., Zhao, H., Li, P., Sun, S., Lai, H., Guo, Q., & Shang, J. (2025). Effects of vegetation restoration type on abundant and scarce soil microbial taxa in a loess plateau mining area. Agronomy, 15(6), 1383. https://doi.org/10.3390/agronomy15061383
32. Misebo, A. M. (2022). Soil Carbon Sequestration in Novel Ecosystems at Post-Mine Sites—A New Insight into the Determination of Key Factors in the Restoration of Terrestrial Ecosystems. Forests, 13(1), 63–63. https://doi.org/10.3390/f13010063
33. Morel, J.-L., Chenu, C., & Lorenz, K. (2015). Ecosystem services provided by soils of urban, industrial, traffic, mining, and military areas (SUITMAs). J. Soils Sediments, 15, 1659–1666. https://doi.org/10.1007/s11368-014-0926-0

34. Moreno, J. L., Bastida, F., Ros, M., Hernández, T., & García, C. (2009). Soil organic carbon buffers heavy metal contamination on semiarid soils: effects of different metal threshold levels on soil microbial activity. European Journal of Soil Biology, 45(3), 220–228. https://doi.org/10.1016/J.EJSOBI.2009.02.004
35. Mühlbachová, G., Sagova-Mareckova, M., Omelka, M., Száková, J., & Tlustoš, P. (2015). The influence of soil organic carbon on interactions between microbial parameters and metal concentrations at a long-term contaminated site. Science of The Total Environment, 502, 218–223. https://doi.org/10.1016/J.SCITOTENV.2014.08.079
36. Nathanail, C. P. (2011). Sustainable Brownfield Regeneration. 1079–1104. https://doi.org/10.1007/978-90-481-9757-6_25
37. Naylor, D., Sadler, N., Bhattacharjee, A., Graham, E. B., Anderton, C. R., McClure, R., Lipton, M., Hofmockel, K. S., & Jansson, J. K. (2020). Soil microbiomes under climate change and implications for carbon cycling. Annual Review of Environment and Resources, 45, 29–59.
38. Naz, M., Dai, Z.-C., Hussain, S., Tariq, M., Danish, S., Khan, I., Qi, S.-S., & Du, D. (2022). The soil pH and heavy metals revealed their impact on soil microbial community. Journal of Environmental Management, 321, 115770–115770. https://doi.org/10.1016/j.jenvman.2022.115770
39. Ngatia, L. W., Moriasi, D., Grace, J. M., Fu, R., Gardner, C. S., & Taylor, R. W. (2021). Land use change affects soil organic carbon: An indicator of soil health. 2021, 1–15. https://doi.org/10.5772/INTECHOPEN.95764
40. Peng, J., Liu, H. K., Hu, Y., Sun, Y., Liu, Q., Li, J., & Dong, Y. (2022). Shift in soil bacterial communities from K- to r-strategists facilitates adaptation to grassland degradation. Land Degradation & Development, 33(12), 2076–2091. https://doi.org/10.1002/ldr.4304
41. Preston, M. D., Brummell, M. E., Smenderovac, E., Rantala-Sykes, B., Rumney, R. H. M., Sherman, G., Basiliko, N., Beckett, P., & Hebert, M. (2020). Tree restoration and ecosystem carbon storage in an acid and metal impacted landscape: Chronosequence and resampling approaches. Forest Ecology and Management, 463, 118012. https://doi.org/10.1016/J.FORECO.2020.118012
42. Qi, Q., Hu, C., Lin, J., Wang, X., Tang, C. C., Dai, Z., & Xu, J. (2022). Contamination with multiple heavy metals decreases microbial diversity and favors generalists as the keystones in microbial occurrence networks. Environmental Pollution, 306, 119406–119406. https://doi.org/10.1016/j.envpol.2022.119406
43. Rees, F., Dagois, R., Derrien, D., Fiorelli, J.-L., Watteau, F., Morel, J.-L., Schwartz, C., Simonnot, M.-O., & Séré, G. (2019). Storage of carbon in constructed technosols: in situ monitoring over a decade. Geoderma, 337, 641–648. https://doi.org/10.1016/j.geoderma.2018.10.009
44. Rumney, R. H. M., Preston, M. D., Jones, T. A., Jones, T. A., Basiliko, N., & Gunn, J. M. (2021). Soil amendment improves carbon sequestration by trees on severely damaged acid and metal impacted landscape, but total storage remains low. Forest Ecology and Management, 483, 118896. https://doi.org/10.1016/J.FORECO.2020.118896
45. Salome, C., Nunan, N., Pouteau, V., Lerch, T. Z., & Chenu, C. (2010). Carbon dynamics in topsoil and in subsoil may be controlled by different regulatory mechanisms. Global Change Biology, 16(1), 416–

426. https://doi.org/10.1111/j.1365-2486.2009.01884.x

46. Sanderman, J., Hengl, T., & Fiske, G. J. (2017). Soil carbon debt of 12,000 years of human land use. Proceedings of the National Academy of Sciences of the United States of America, 114(36), 9575–9580. https://doi.org/10.1073/PNAS.1706103114
47. Semple, K. T., Doick, K. J., Wick, L. Y., & Harms, H. (2007). Microbial interactions with organic contaminants in soil: definitions, processes and measurement. Environmental Pollution, 150(1), 166–176. https://doi.org/10.1016/J.ENVPOL.2007.07.023
48. Song, Y., Kirkwood, N., Maksimovic, C., Zheng, X., O'Connor, D., Jin, Y., & Hou, D. (2019). Nature based solutions for contaminated land remediation and brownfield redevelopment in cities: A review. Science of The Total Environment, 663, 568–579. https://doi.org/10.1016/J.SCITOTENV.2019.01.347
49. Soussana, J.-F., Lutfalla, S., Ehrhardt, F., Rosenstock, T. S., Lamanna, C., Havlik, P., Richards, M., Wollenberg, E. K., Chotte, J.-L., Torquebiau, E., & Ciais, P. (2019). Matching policy and science: Rationale for the '4 per 1000 - soils for food security and climate' initiative. Soil & Tillage Research, 188, 3–15. https://doi.org/10.1016/J.STILL.2017.12.002
50. VCS. (2023). Methodology for Improved Agricultural Land Management. https://verra.org/methodologies/vm0042-methodology-for-improved-agricultural-land-management-v2-0/
51. Wan, Y., Chen, S., Liu, J., & Jin, L. (2024). Brownfield-related studies in the context of climate change: A comprehensive review and future prospects. Heliyon. https://doi.org/10.1016/j.heliyon.2024.e25784
52. Xiao, C., Gong, Y., Pei, X., Chen, H., Li, S., Lü, C., Chen, L., Xiaoxian, Z., Zheng, J., & Xie, Y. (2024). Impacts of Land-Use Change from Primary Forest to Farmland on the Storage of Soil Organic Carbon. Applied Sciences, 14(11), 4736–4736. https://doi.org/10.3390/app14114736
53. Xiao, Z., Duan, C., Li, S., Chen, J., Peng, C., Che, R., Liu, C., Huang, Y., Mei, R., Xu, L., & Luo, P. (2023). The microbial mechanisms by which long-term heavy metal contamination affects soil organic carbon levels. Chemosphere, 139770–139770. https://doi.org/10.1016/j.chemosphere.2023.139770
54. Xu, S., Sheng, C., & Tian, C. (2020). Changing soil carbon: Influencing factors, sequestration strategy and research direction. Carbon Balance Manag., 15, 1–9. https://doi.org/10.1186/s13021-020-0137-5
55. Yan, Z.-X., Li, Y., Peng, S.-Y., Wei, L., Zhang, B., Deng, X.-Y., Zhong, M., & Cheng, X. (2024). Cadmium biosorption and mechanism investigation using two cadmium-tolerant microorganisms isolated from rhizosphere soil of rice. Journal of Hazardous Materials, 470, Article 134134. https://doi.org/10.1016/j.jhazmat.2024.134134
56. Yang, Y., Yang, Y., Yang, Y., Hobbie, S. E., Hernandez, R. R., Fargione, J., Grodsky, S. M., Tilman, D., Tilman, D., Zhu, Y. G., & Luo, Y. (2020). Restoring Abandoned Farmland to Mitigate Climate Change on a Full Earth. 3(2), 176–186. https://doi.org/10.1016/J.ONEEAR.2020.07.019
57. Yuan, C., Wu, F., Wu, Q., Fornara, D. A., Hedenec, P., Peng, Y., Zhu, G., Zhao, Z., & Yue, K. (2023). Vegetation restoration effects on soil carbon and nutrient concentrations and enzymatic activities in post-mining lands are mediated by mine type, climate, and former soil properties. Science of The Total Environment, 879, 163059–163059. https://doi.org/10.1016/j.scitotenv.2023.163059

58. Zeng, K., Huang, X., Guo, J., Dai, C., He, C., Chen, H., & Xin, G. (2024). Microbial-driven mechanisms for the effects of heavy metals on soil organic carbon storage: A global analysis. Environment International, 184, 108467–108467. https://doi.org/10.1016/j.envint.2024.108467

Figures

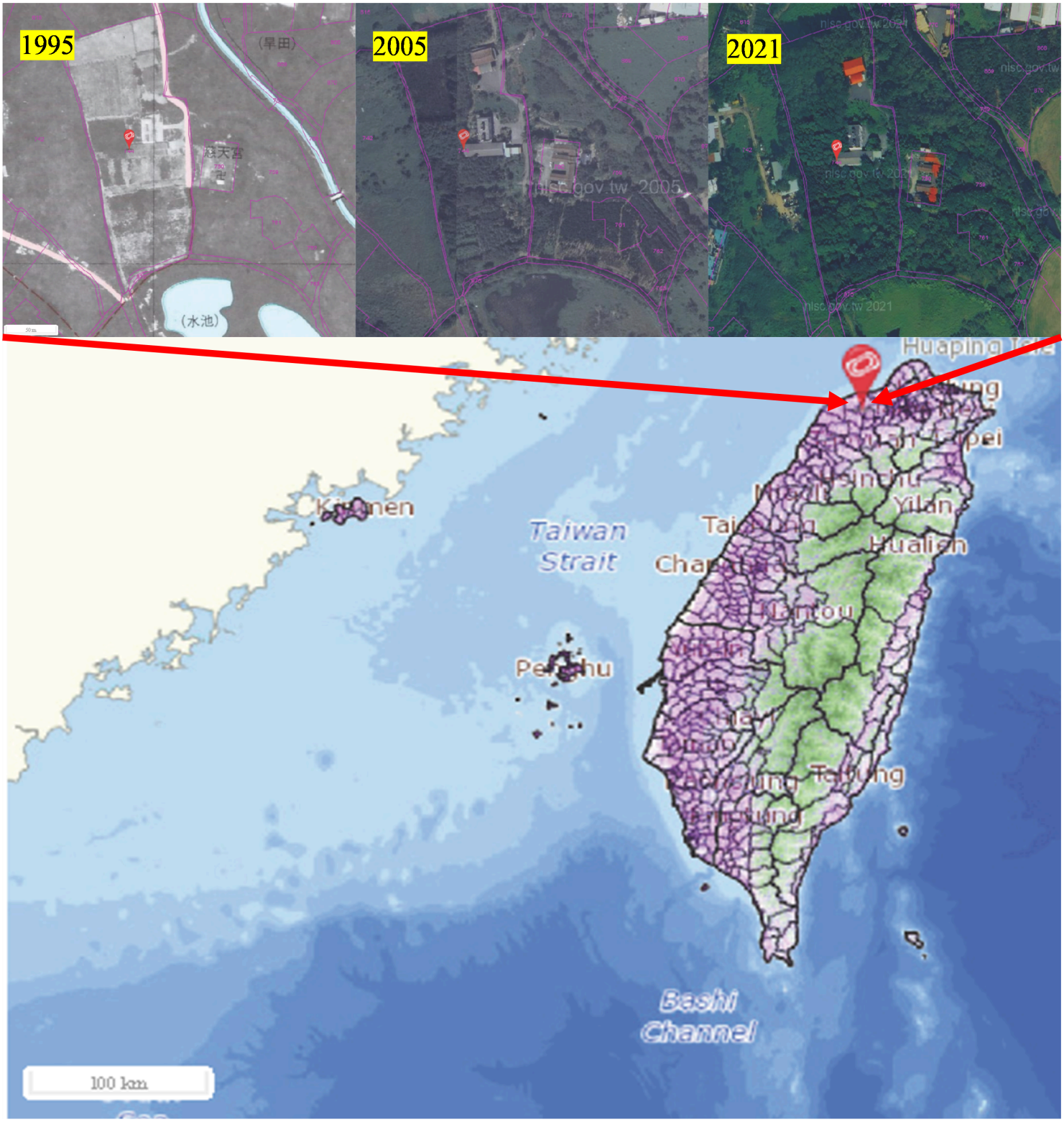


Figure 1

Landscape alterations of the studied area by aerial photograph

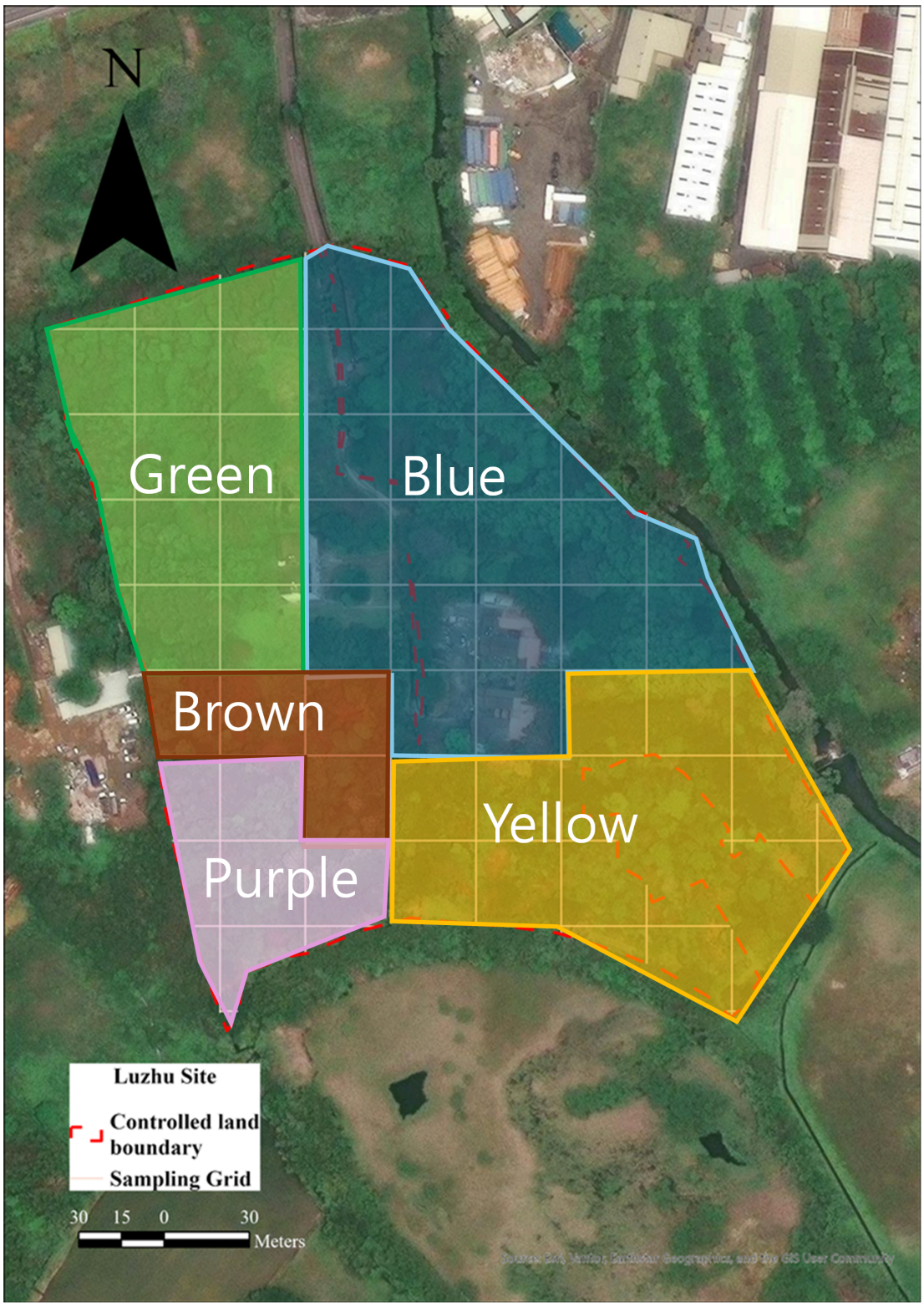


Figure 2

Zonal delineation of the investigation zones based on vegetation planting planning and human intervention

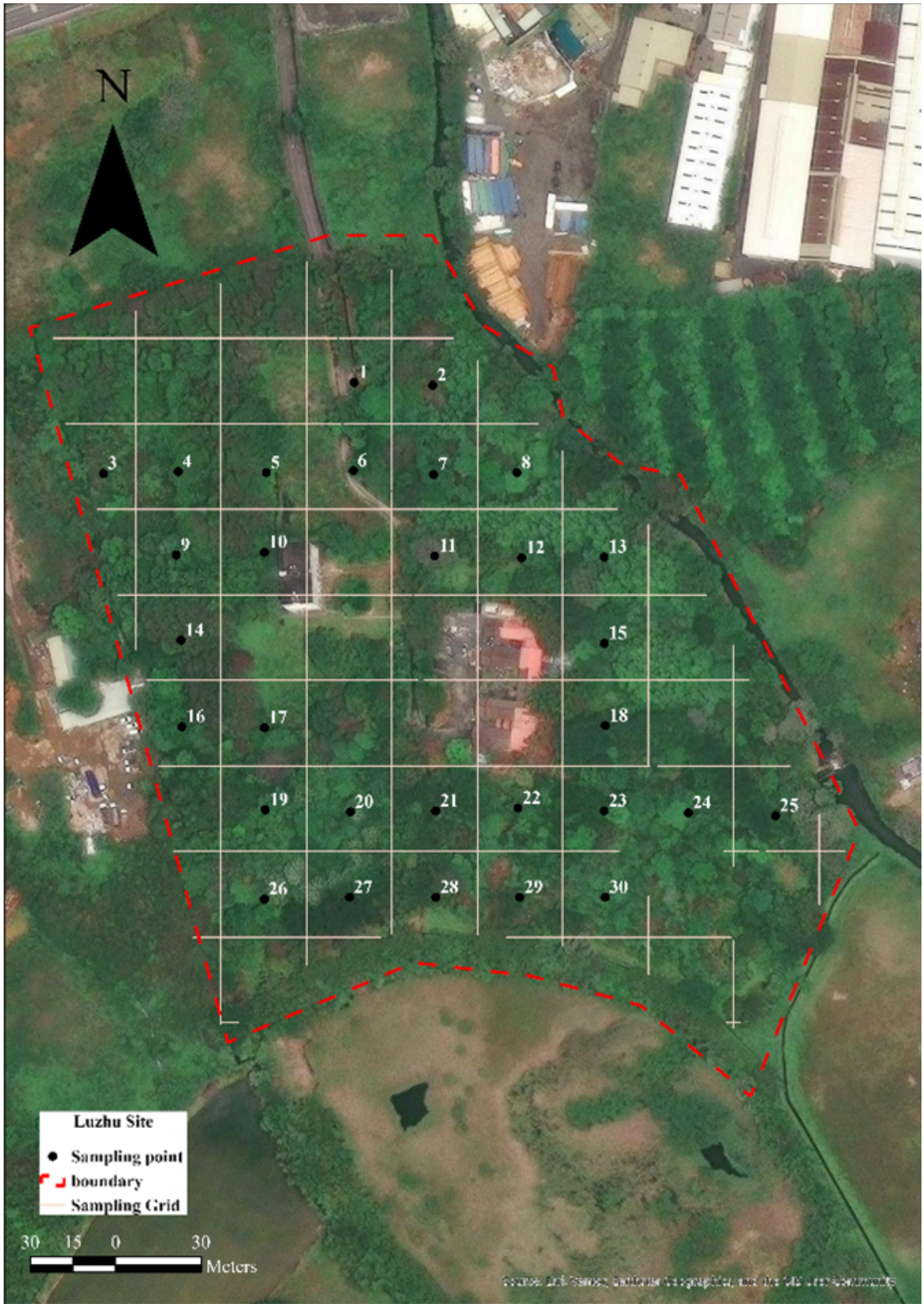


Figure 3

Grid-based sampling layout for soil, microbial activity, and vegetation investigation

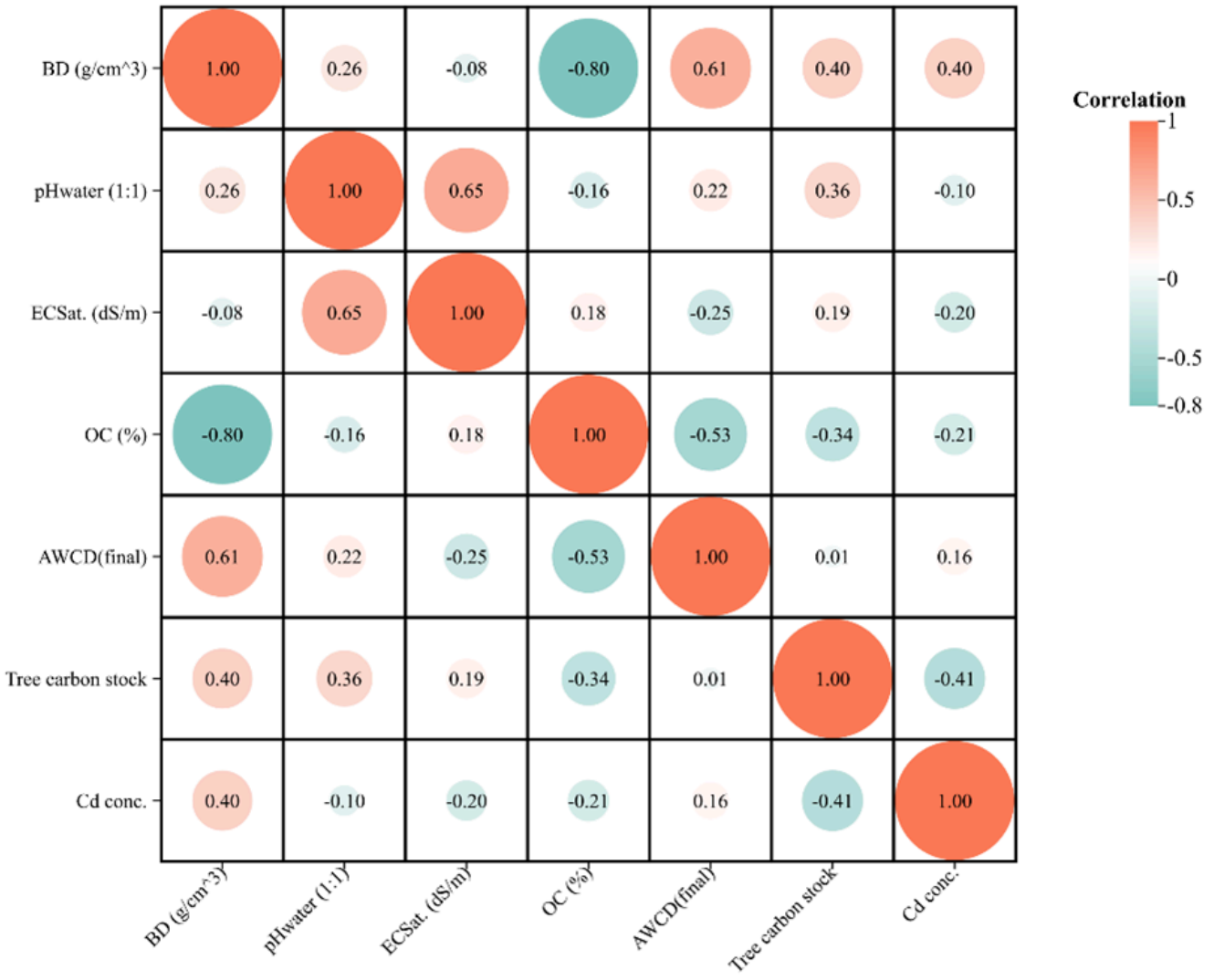


Figure 4

Correlation analysis between soil physicochemical properties, cadmium concentration, and AWCD in the topsoil

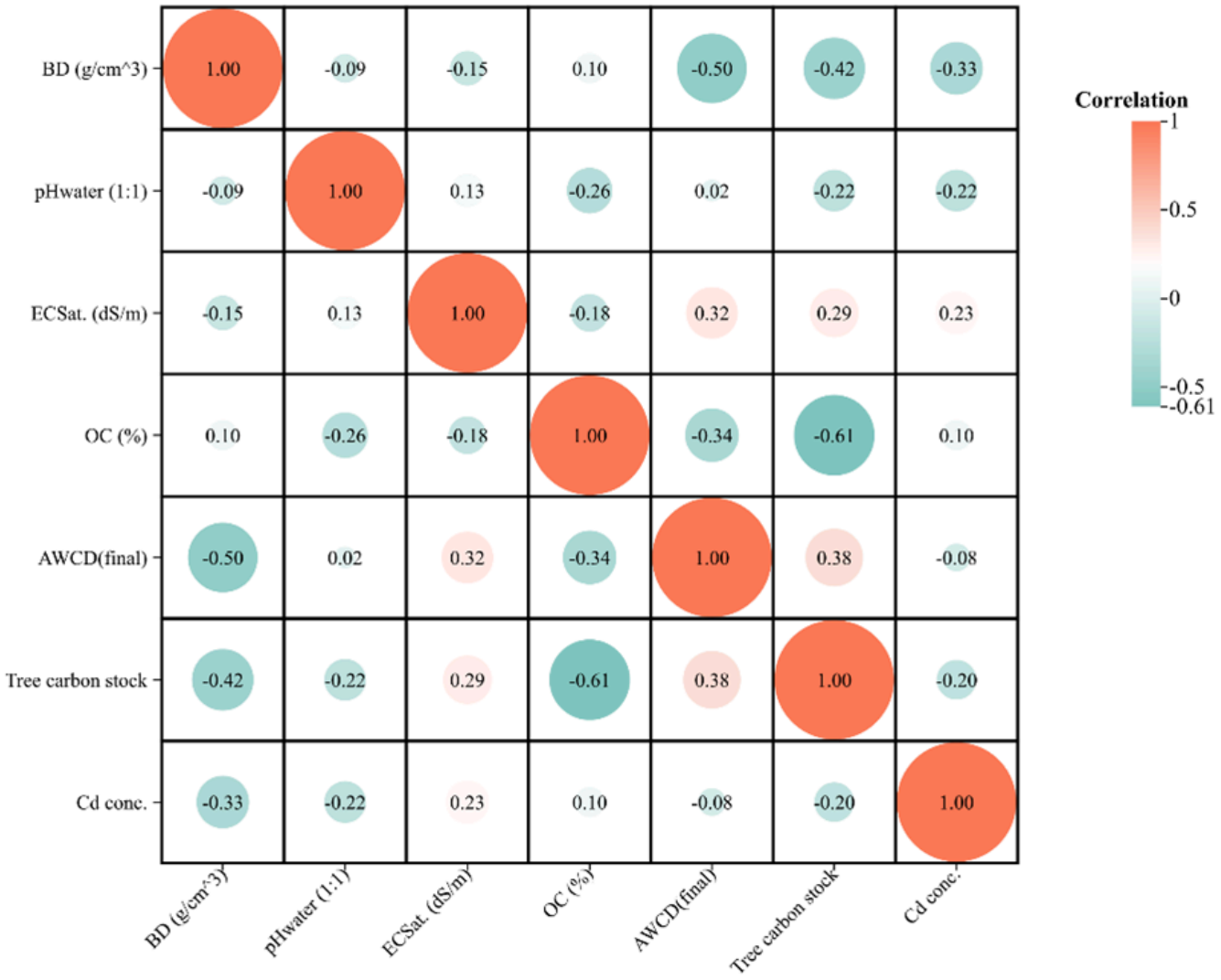
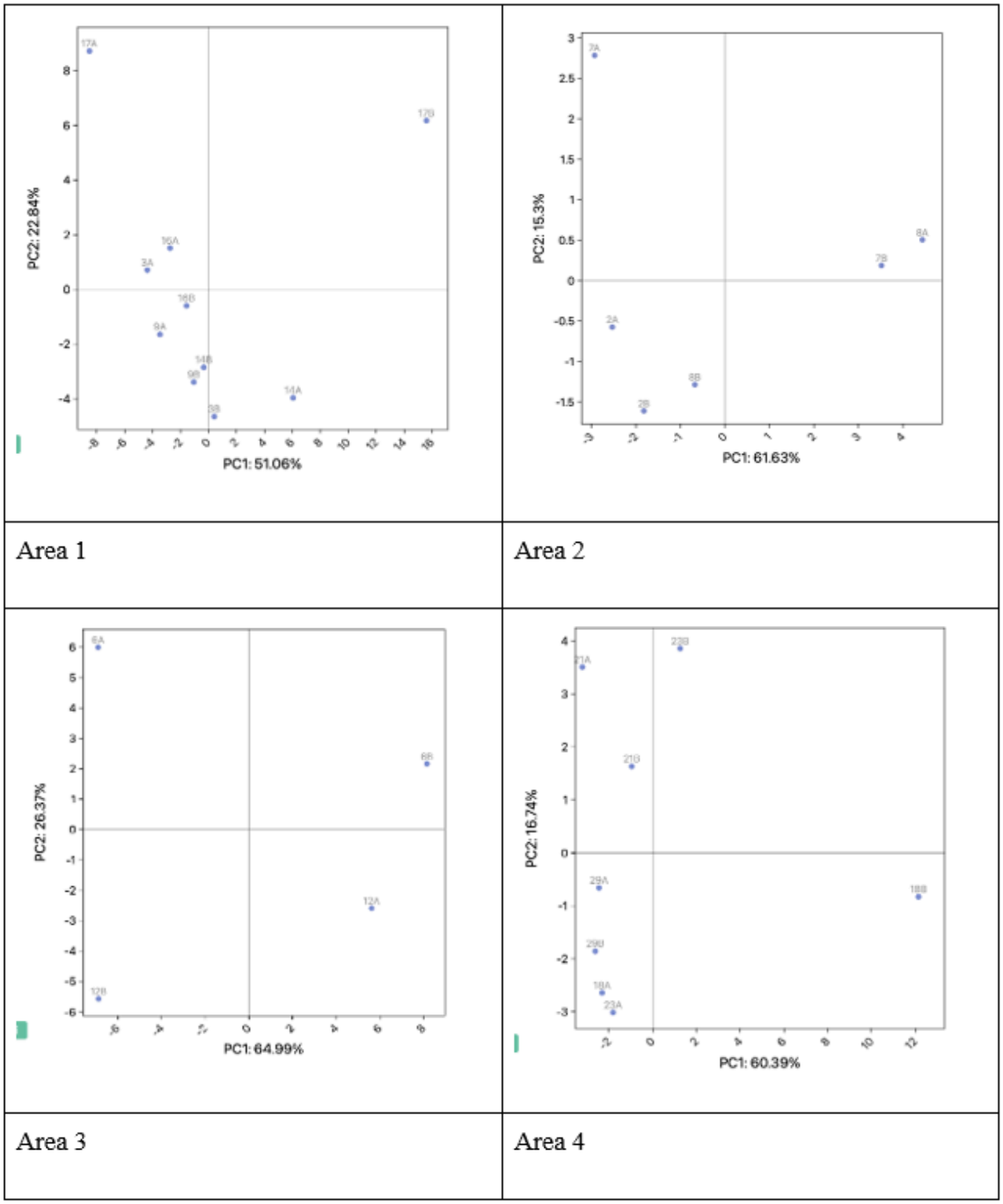


Figure 5

Correlation analysis between soil physicochemical properties, cadmium concentration, and AWCD in the subsoil



Area 1 | Area 2

Area 3 | Area 4

Figure 6

Principal component analysis (PCA) of soil microbial functional metabolic diversity based on AWCD carbon source utilization profiles

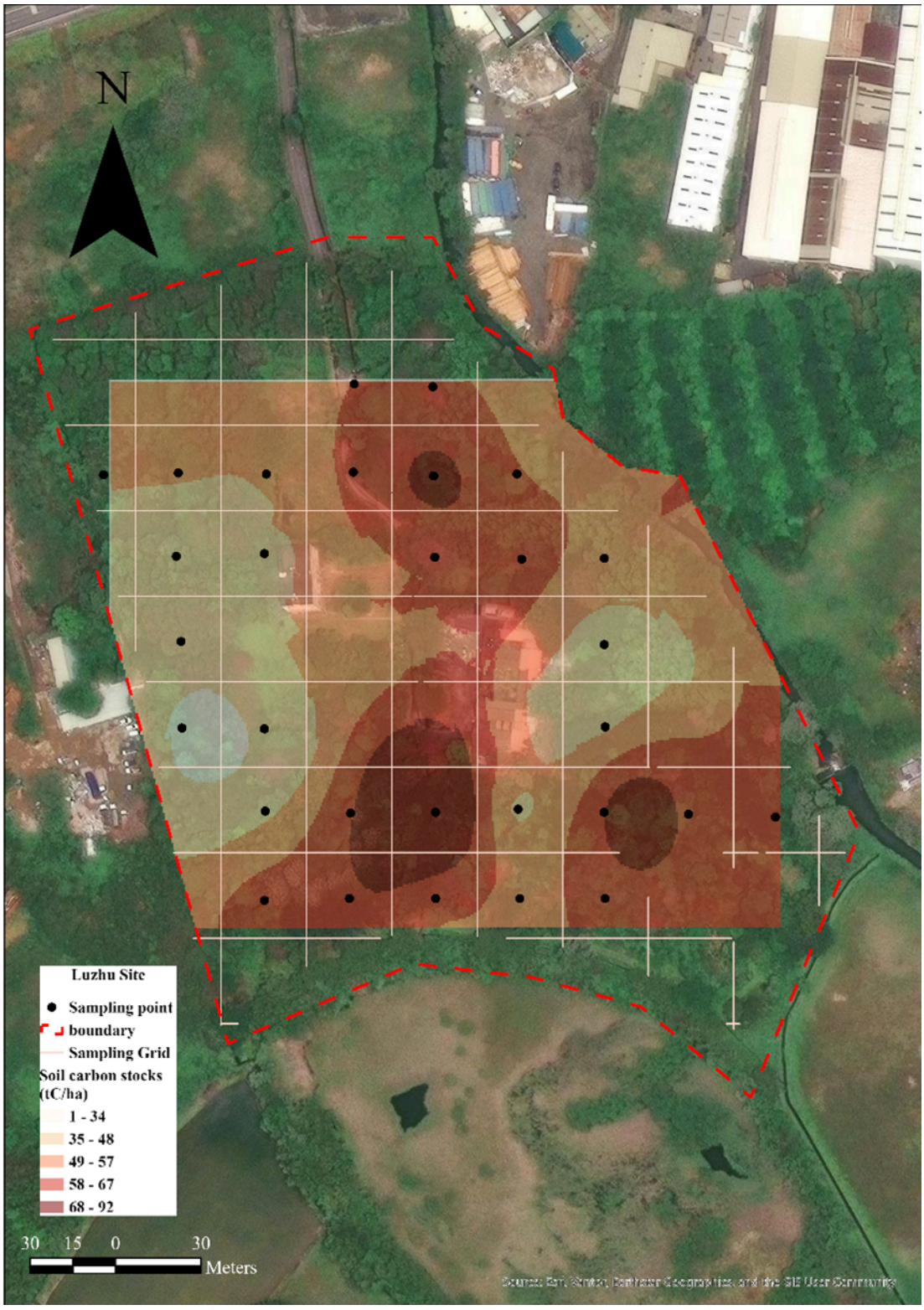


Figure 7

Soil organic carbon stocks map in studied area

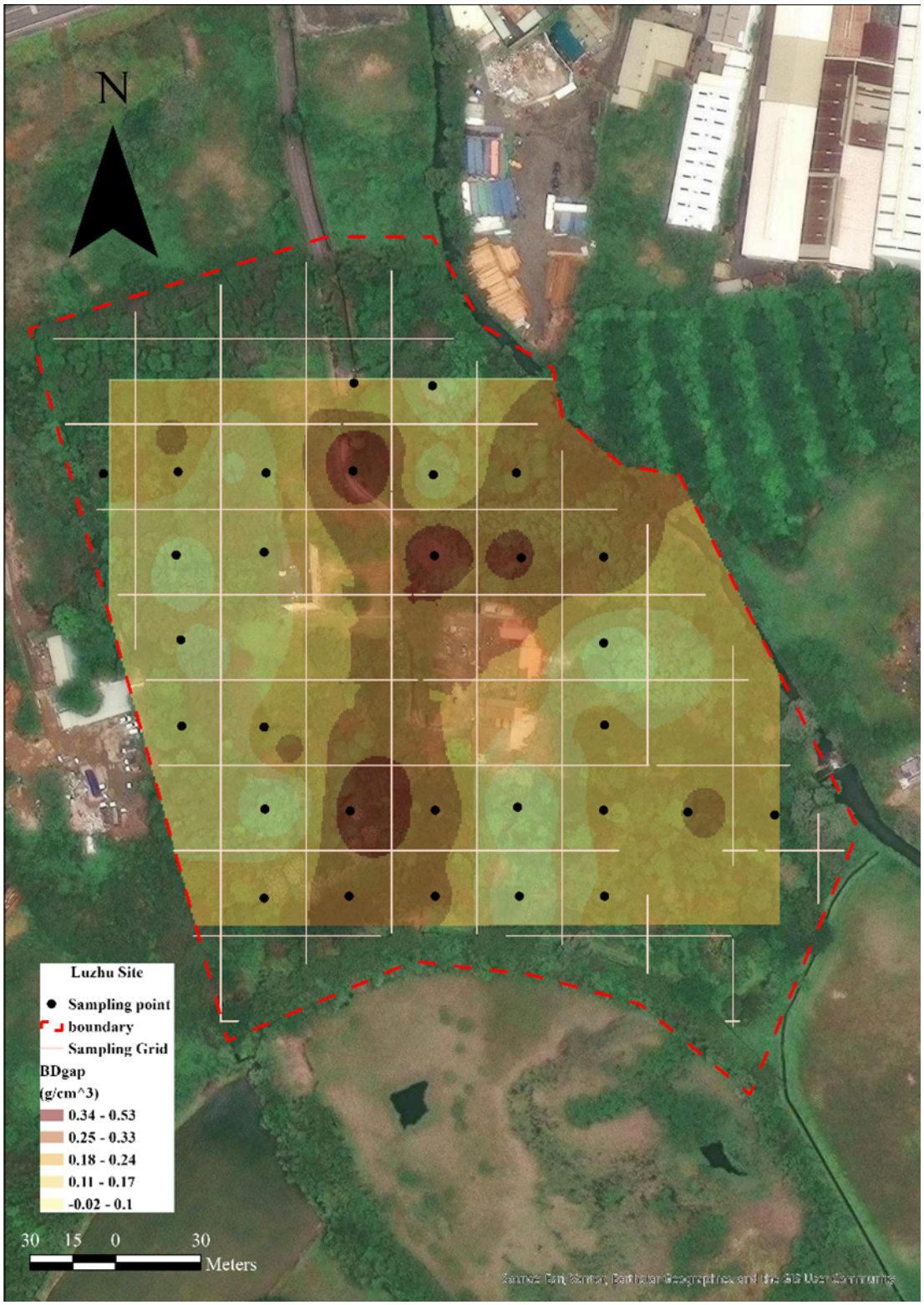


Figure 8

Map of soil bulk density differentials between topsoil and subsoil layers

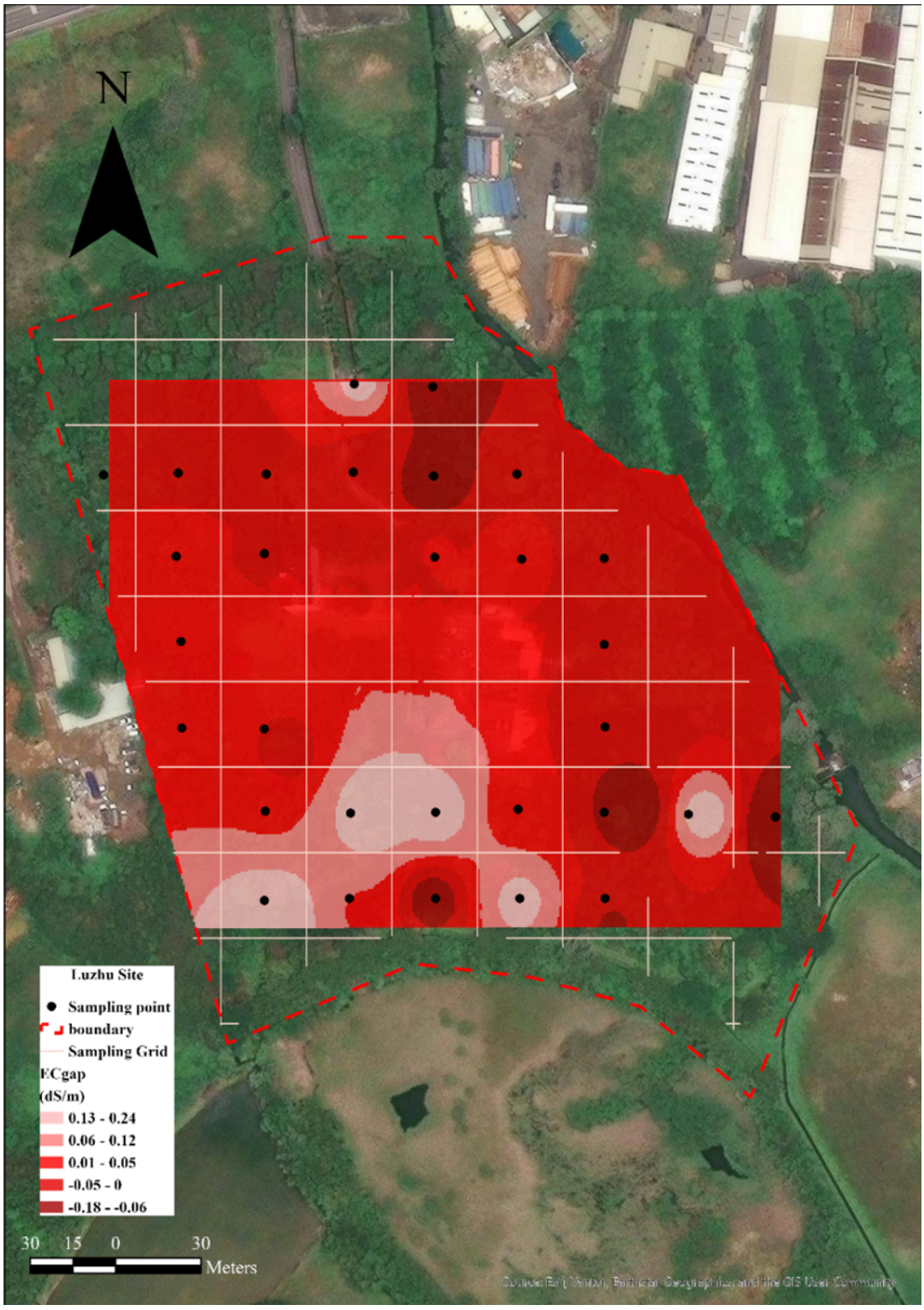


Figure 9

Map of electrical conductivity differentials between topsoil and subsoil layers

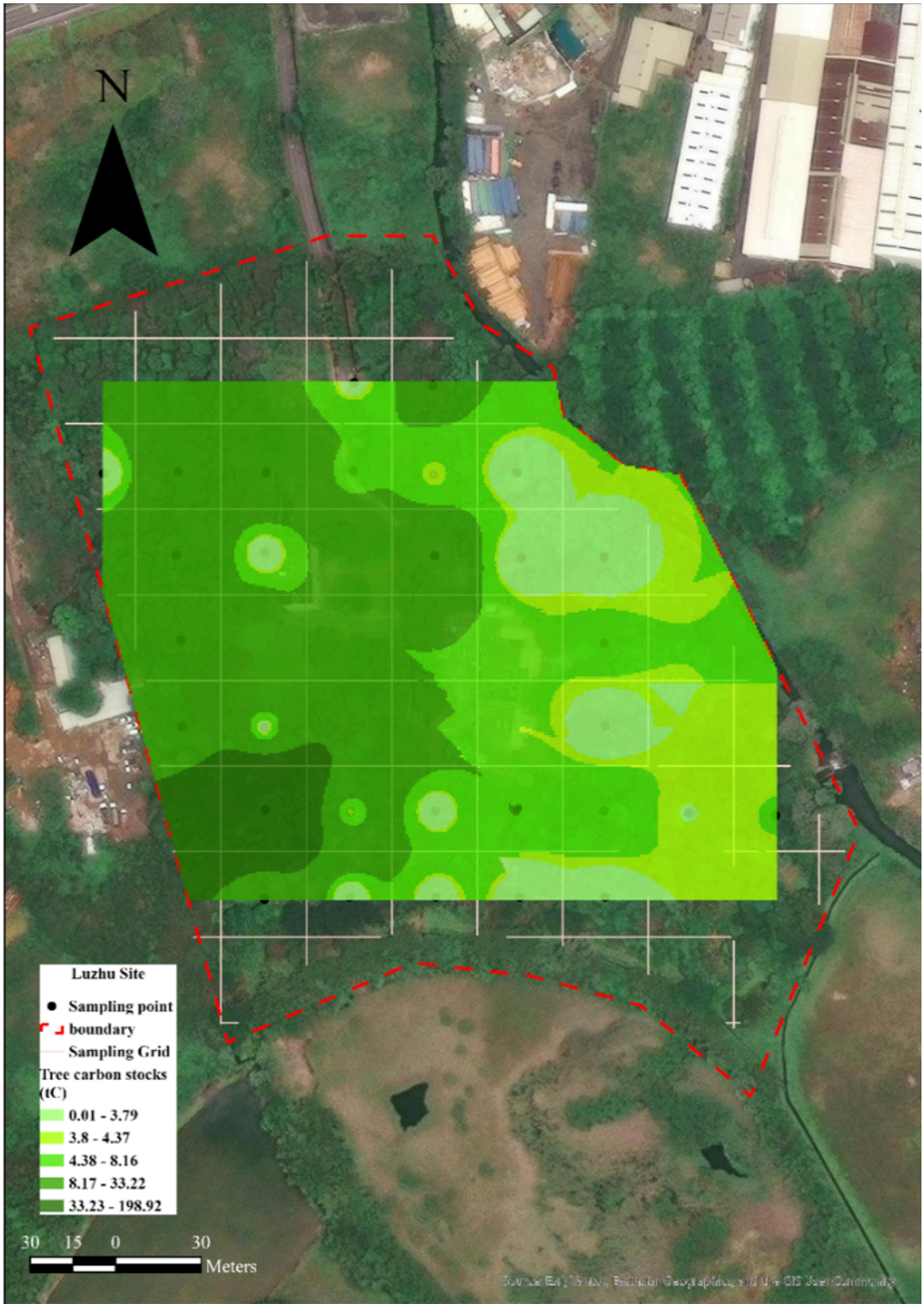


Figure 10

Tree carbon stocks map within the long-term phytoremediation

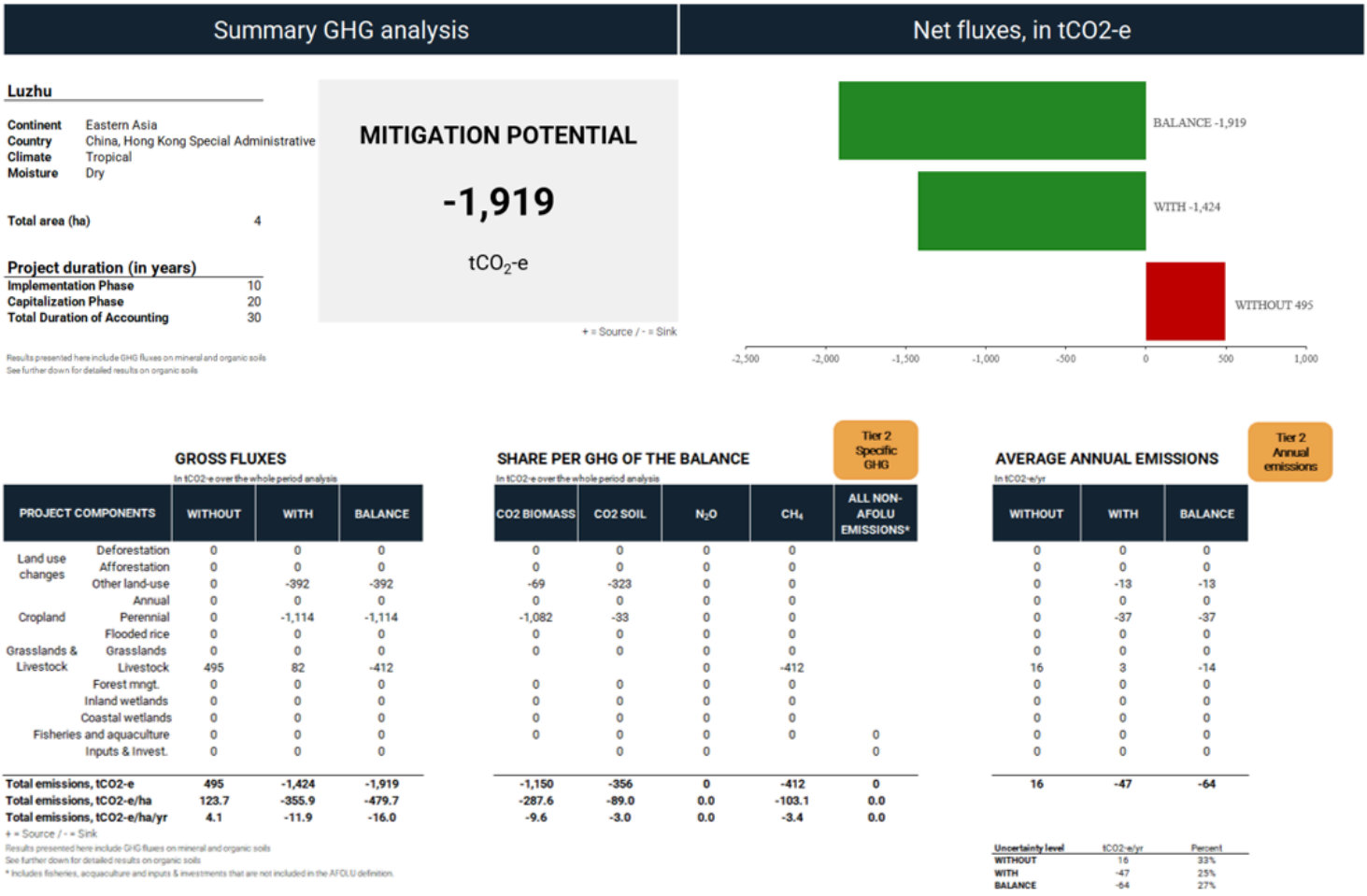


Figure 11

Net carbon balance and sequestration potential using EX-ACT Tool